The liquid regime of waxy oils suspensions: A Magnetic Resonance Velocimetry Analysis

Diogo E.V. Andrade, Maude Ferrari, Philippe Coussot

The liquid regime of waxy oils suspensions: A Magnetic Resonance Velocimetry Analysis

Diogo E. V. ANDRADE[a], Maude Ferrari[b], Philippe COUSSOT[a,*]

[a] Laboratoire Navier (ENPC, Univ Gustave Eiffel, CNRS), 14-20 Bd Newton, 77447 Marne-la-Vallée, France.

[b] Université de Lorraine, CNRS, LEMTA, 2 Avenue de la Forêt de Haye, F-54000 Nancy, France

[*]Corresponding author. E-mail: philippe.coussot@ifsttar.fr

Abstract: In view of better understanding the properties of waxy crude oils of great practical importance, we study the rheological behavior evolution of model waxy suspensions during transient shear tests, and its variation with concentration in a wide range. Macroscopic tests show a strong destructuring process with the increasing imposed shear rate (starting from rest), while negligible restructuring is observed during shear rate decrease. MRI (Magnetic Resonance Imaging) velocimetry of the suspension during the same tests allow to observe that, in most of the concentration range tested, the material flows only in a limited thickness close to the inner cylinder, and the thickness of this shear-band decreases for increasing concentration but marginally evolves as the apparent shear rate is widely increased then decreased. This means that the extent of the liquid region is governed by the initial start-up flow conditions, and the apparent viscosity variations during the next steps (at other shear rate values) are not associated with an increase of the flowing region but with the evolution of the structure in the liquid region. For the specific case of the lowest wax content analyzed, the thickness of the unsheared region decreases considerably after shearing at a high shear rate. In this case the torque balance in the sample is capable of overcoming the yield stress of the unsheared region. We also show that despite very different (initial) elastic moduli and yield stresses in the solid regime (a factor of several orders of magnitude over the whole range of concentration), we essentially have the same power-law behavior of the fluid in the shear-band, even when the shear-band thickness is close to the particle size.

Keywords: Waxy oils, Liquid Regime, MRI, Shear banding

1. INTRODUCTION

Crude oils are essentially composed by hydrocarbons which, in the reservoir conditions, at high temperatures (around 60 to 150 °C) and pressures (around 50 to 150 MPa), are in the liquid state. During the production and transportation in the offshore scenario, the crude oils are carried in pipelines, which can be hundreds of kilometers long, and are in contact with the seabed, a low temperature environment (around 4°C). In the course of flow in the pipelines, the oil loses heat to the environment, the solubility of high molecular weight components in the oil decreases, and eventually the temperature can reach the WAT (Wax Appearance Temperature), for which the first solid paraffin crystals precipitate in the oil [1]. When flow is stopped for programmed maintenance or some issue in the production, the precipitated crystals can form a network, entrap the oil, and give a structure to the material. In order to break this structure and start-up the flow, it is necessary

to impose a pressure much higher than the steady-state pressure used in the usual flow. To avoid damage to the pipelines and guarantee enough pump pressure to break this structured material, the system must be designed to support these high pressures. On the other hand, if the problems related to the flow assurance are overestimated in the conceptual phase, the project of pipelines and pumps can be economically prohibited. These different points highlight the importance of understanding the mechanical properties of the structured waxy oil, the breakage process and how the flow evolves after the pipeline restart.

Waxy oils are thermal and shear-history-dependent materials. In other words, it is not possible to determine the mechanical properties of the waxy oils just knowing the current temperature, pressure and composition of the sample. In particular, to have some idea of the rheological properties of these materials, one has to be aware of the oil initial cooling temperature [2–4], the cooling rate [5,6], the shear [7–9] and the subsequent resting time [10,11] experienced by the material prior to the moment of analysis. Some works related the amount and morphology of the crystals with the rheological properties of the material: it was shown that the thermal and shear histories can affect the crystallization process (nucleation and growth of the crystals) and, as a consequence, the rheological behavior of the material [6,7]. On the other hand, it is not a straightforward task to predict the critical stress to break-up the material and the behavior of the material in the liquid regime even when the composition of the waxy oil, the thermal and shear histories are well controlled in rheometrical tests. It seems that determining the morphology of the crystals by means of different microscopic techniques and combining this information with the macroscopic behavior obtained in conventional rheometry [5,6,12,13] is not enough to fully understand the solid-liquid transition or the liquid regime. The influence of crystal morphology and size on the material structure strength is still an open question in the literature since some authors state that the critical stress and the elastic modulus increases with the size of the crystals [7], other authors claim the opposite [5], and some papers show a non-monotonic influence of the length of the crystals and the stress required to start-up the flow [6,12]. Regarding the liquid regime, it is interesting to note that while some authors state that increasing the size of the crystals decreases the apparent viscosity of the waxy oil [5], other authors argue that the aggregation of the crystals reduces the oil viscosity [13], and some researchers claim that the morphology of the crystals is not the point in the analysis of the waxy oil viscosity but the interactions between the crystals [14]. It seems that to further understand the relation between crystal's morphology and rheological properties, the analysis of the local deformation and velocity inside the gap can be a useful information.

An approach that has been used only in a few previous works and which can provide valuable insights in this field is velocimetry, since this provides some information on how the material behaves locally and instantaneously and, then, one may relate the macroscopic measurements with the effective deformations. So far, local velocities and deformations in well-controlled waxy oils experiments have been measured using PIV (Particle Imaging Velocimetry) in pipeline flow [15], Rheo-PIV [16,17] and MRI (Magnetic Resonance Imaging) velocimetry in rheometrical tests [18]. El-Gendy et al. [15] showed a plug-like flow in the pipeline restart in which just a small portion of the material close to the walls was broken. Important wall slip effects when smooth surface geometry is used and erosion in the microstructure were observed by Dimitriou et al.

[17]. Shear banding and material instabilities in the liquid regime at low imposed shear rates were reported by Dimitiou and Mckinley [16]. The irreversibility of the material behavior after determined shear history was demonstrated by Mendes et al. [18]. Despite such advances in this field, a further knowledge of the structure breakage process and the behavior of the material after the start-up remains an open and important field in the flow assurance area.

In that aim we suggest it could be very instructive to study the variations of the rheological behavior and flow characteristics of these systems as a function of the solid concentration of the suspension. We can indeed expect that a variation of some intrinsic characteristics of the fluid can lead to some progressive regime changes, and analyzing these trends can provide a better understanding of the origin of flow characteristics. In a previous paper [19] it was shown that above a critical value the material yield stress increases rapidly with the concentration, due to a solid structure made up of bonds that connect the crystals, entrap the oil and give a solid behavior to the material with high elastic modulus (up to 10^6 Pa for the model oil analyzed) and yield stress (up to 10^4 Pa for the thermal history analyzed). For some concentrations the elastic modulus and the yield stress appeared to decrease by more than three orders of magnitude during the solid-liquid transition. It was also suggested [19] that in the liquid regime the material exhibits the behavior of a simple suspension but in some cases shear-banding was observed, which precludes a reliable analysis of the effective shear rate and of transient regimes.

In order to address these questions, we analyze the liquid regime of waxy oils suspensions by means of MRI velocimetry. This specific technique was used by some authors to study the behavior of yield stress fluids [20], thixotropic materials [21–23] and, as reported above, was already employed for waxy oil suspensions [18]. In that work [18], it was shown that the flow curve of the material is affected by the maximum shear rate experienced by the fluid. In other words, the authors showed that every time a new maximum shear rate is imposed, the material presents a new rheological liquid behavior. However, the authors just analyzed the behavior of a suspension with low wax concentration in oil.

Here, we focus on a suspension cooled at rest and we look at the impact of the wax concentration on the material behavior following a single and simple protocol (progressive increase then decrease of the velocity), so that we can identify more clearly the behavior in the liquid regime during transient stages for the different concentrations. We finally show that depending on the wax concentration, the deformed and undeformed regions (shear bands) can be a critical factor to be taken into consideration in the analysis of the rheometrical measurements. Although these findings cannot be directly transferred to the start-up flow of waxy oil and waxy crude oils in pipelines due to the influence of axial coordinate which complicates the analysis, our results show that shear band is an important issue to be taken into consideration in pipelines flows, a vital point in the oil and gas industry.

2. EXPERIMENTAL SECTION

The waxy oil was prepared by adding solid Paraffin (Sigma Aldrich 330779 CAS-No: 8042-47-5) in mineral oil (Sigma Aldrich 377212 CAS-No: 8002-74-2) and putting the mixture in the oven at 60 °C in order to dissolve all the paraffin in the oil. Six different concentrations of paraffin in oil were analyzed: 6, 7, 8, 10, 12 and 15 wt.%. It is worth mentioning that in this range the elastic modulus first increases with concentration as for a percolating structure and beyond 10 wt.% the elastic modulus reaches a plateau while the yield stress further increases. The values of elastic modulus, measured from oscillations of very small amplitude, and yield stress, measured through creep tests at low shear rate, are recalled in Figure A2 (Appendix). These features are associated with a similar structure for different concentrations, except beyond 10% (See Figure A2 and ref. [19]). Moreover, an abrupt start-up flow beyond the yield stress, leading to very fast flow after the breakage, was observed. An apparent similar behavior was reported for different concentrations but possible shear-banding could significantly affect the analysis at large concentrations (see [19]). The analysis of different concentrations is important since the wax content in real crude oil can vary in a wide range (for example, for several Brazilian crude oil the wax content varied from 5 up to 25 wt% see [24]).

Here, for all the measurements we used a Couette geometry (see Figure 1) made of Polypropylene with 31 mm diameter for the cup, with 15 mm diameter and 75 mm of height for the internal rotating cylinder. The geometries have knurled rough surface to avoid wall slip [25]. The sample was poured into the cup at 60 °C, then the geometry was inserted in the equipment and the material was cooled statically by natural convection until the ambient temperature is reached (~25 °C). The ambient temperature was controlled by the air conditioning system and the resting time at the final temperature was one hour for all the experiments. It is well known that the thermal history (e.g., cooling rate) affects the solid behavior of waxy oils [6], but in these experiments we are keeping always the same sample preparation procedure, so that is possible to analyze the influence of concentration of paraffin in the liquid regime of the waxy oils independently of the thermal history. The experiments were performed in the MRI equipment (see Section 2.1) in order to measure the velocity profile as a function of the rotation velocity, and then the identical procedures were repeated with the same geometry in a rotational Malvern Kinexus Pro+ rheometer to measure the torque in all the analyzed cases.

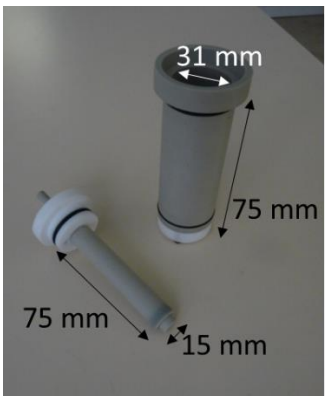

Figure 1. Polypropylene Couette geometry used to perform the experiments in the MRI and in the conventional rheometer.

We choose to follow a single protocol for all the tests and materials. This protocol allows to observe the main transient and steady trends of the rheological behavior in the liquid regime. It consists to suddenly apply, to the material initially left a long time at rest at a temperature for which it has reached a solid state at

equilibrium, a series of increasing then decreasing values of rotation velocities. Moreover, before the decreasing stage a much higher rotation velocity was applied for some time. In such a way we test the start-up flow characteristics from rest, then the possible destructuring process varying with the imposed shearing, and finally the possible restructuring process during a decrease of the imposed rate of shear.

More precisely, the rotation velocities analyzed were: 6, 9, 15, 24 and 39 RPM (which correspond to the range of the measured range of the MRI equipment). The control procedure was performed by the start-up experiment at the lowest velocity (6 RPM), then the rotation was kept during five minutes and then increased to the next rotation velocity again for five minutes. After the end of the highest possible measuring rotation velocity (39 RPM), the velocity was increased to 300 RPM, which is the maximum velocity that may be imposed in the MRI equipment without taking any image. The sample was sheared at the maximum velocity during five minutes and then rotation velocity was decreased to the same values used during the increasing phase. This procedure is presented in Figure 2 (dashed line). In order to get an idea of the magnitude of shearing, using the assumption that the sample is flowing in all the gap (8 mm), the expected apparent shear rate would be in the order of 5 s^{-1} for the imposed velocity of 300 RPM.

2.1 MRI velocimetry

The velocity profiles are obtained by the MRI technique [23,26] with a Bruker Avance III 600 wide bore spectrometer (magnetic field B = 14.1T, proton resonance frequency = 600 MHz) in LEMTA at Université de Lorraine. The spectrometer is equipped with a gradient system of 45G/m. The spectrometer is fitted with a Rheo-NMR accessory manufactured by Magritek. The micro-imaging probe (MicWB57) used is manufactured by Bruker and it is equipped with a 40-mm-diameter quadrature resonator. Image acquisition was performed using the flow encoding spin-echo sequence. The geometric parameters are as follows: the field of view (FOV) is 1.5 cm×3.5 cm, the thickness slide is 20mm, and the matrix is 256×32 pixels. The velocity profiles obtained have a spatial resolution of about 60 μm. As proposed elsewhere [27] for each 2D flow map, we represent the velocity in each position as a function of its distance to the center of the inner cylinder, then average to finally obtain a single velocity profile for each rotation velocity.

3. RESULTS AND DISCUSSION

3.1 Conventional rheometry

Let us first look at the response of the material during rheometrical tests (Figure 2). Initially (within the first second), the measured torque reaches high values and then it decreases rapidly in time. This fast decrease of the torque, when we keep the constant rotation, is expected since as observed in the previous paper [19] the solid-liquid transition in this system can be understood as a collapse, which explains the fact that the material exhibits a very fast solid-liquid transition. After the initial breakage, the torque keeps decreasing during the five minutes of shearing at this initial rotation velocity. We can see, especially for low values of

rotation velocity and high concentrations, that the torque presents some fluctuations on time. In fact, these fluctuations are rather simple oscillations but with a period which can be typically one order of magnitude smaller than the period of rotation of the tool, and which does not vary proportionally to the rotation velocity. We can conclude that this is not a rheometer control problem or some issue with the geometry since the amplitude of these oscillations decreases when the rotation velocity is increased and, after the maximum rotation velocity of 300 RPM, except for the highest concentrations, i.e. 12 and 15%, the oscillations are not present anymore in the measurements in the decreasing phase. It seems likely that this is due to some heterogeneities remaining in the fluid (maybe some large solid blocks) for some time after the first bonds have been broken in the material. In fact, we will see later that these oscillations are observed in cases for which the sheared region is very small, so that we will be able to discuss further about their origin. Although we keep this observation in mind for the qualitative analysis of the data, we will neglect this aspect for any quantification.

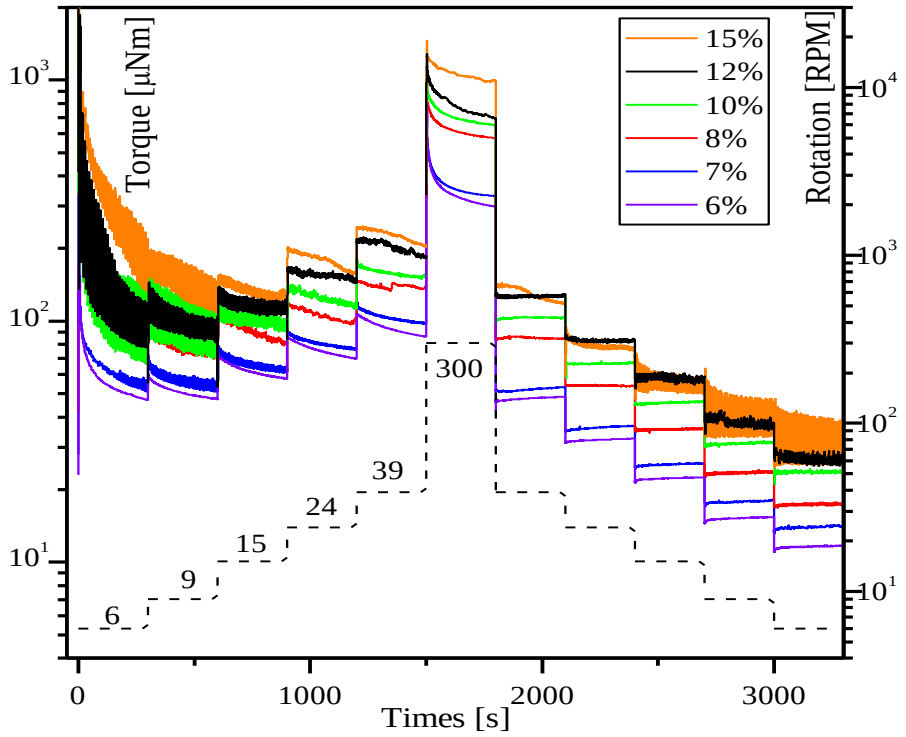

Figure 2. Torque (solid lines) and imposed rotation velocity (dashed line) as a function time for the different concentrations. Each value of rotation was maintained in the sample during 5 minutes. The thicker line aspect corresponds to the fluctuations (see text).

The first fundamental observation is that the torque significantly decreases during the first five minutes of shearing for all the steps during the rotation velocity increasing phase. Thus, it seems that the material is breaking down over time and when a higher rotation is experienced the breakdown process is more pronounced. Finally, we observe that the flow is not in steady state after five minutes of shearing in the increasing phase at any rotation velocities, except at 300 rpm, where the material seems to tend to an equilibrium at the end of the step (see Fig. 2). Then, for each decreasing step, except for 15%, the material almost immediately reaches an equilibrium, with some very slight increase of the stress in time, which might be associated to a slight restructuring trend. It is interesting to note that, roughly speaking, in this decreasing

phase the variation of the torque between two successive steps is similar to the variation of the rotation velocity, which as a first glance can indicate that the viscosity of the material is approximately constant in this analyzed range. These results are consistent with the conclusion that the maximum shear rate imposed to the sample affects the behavior of the material [18], and the measured torque in this increasing phase completely depends on the shear history experienced by the material. We can thus effectively observe that in the decreasing phase the torque values strongly differ from those observed during the increasing phase (see Fig. 2).

Here we carried out such tests for the different concentrations and could observe qualitatively similar trends in the range [6 - 15%] leading to similar interpretations concerning the evolution of the rheological behavior. In addition, it is remarkable that the timing for stress decrease during the increasing phase is roughly independent of the concentration after rescaling by the maximum stress: in a logarithmic scale, the stress vs time curve after a change to a given velocity, are roughly similar (equal by simple vertical shift). Globally speaking, the curves are similar after some rescaling using as parameter the torque measured at the end of 5 minutes of shearing at 300 RPM, this tends to suggest that the destructuring processes are only dependent of the flow history.

In Couette geometries, in the flowing region the shear stress (τ) distribution is given from the momentum balance in the absence of inertia effects:

$$\tau = M/2\pi h r^2 \qquad (1)$$

And from straightforward kinematic considerations, the local shear rate $(\dot{\gamma})$ is related to the rotation velocity through

$$\dot{\gamma} = -r\, d\omega/dr \qquad (2)$$

in which M is the torque, h is the height of the cylinders, r is the position in the radial position and ω is the local rotation velocity of the material. From these results (Figure 2), one could try to make the analysis of the measurements in terms of shear stress vs shear rate using unadvisedly the traditional assumptions to calculate the shear stress ($\tau = M/2\pi h R_1^2$) and the shear rate ($\dot{\gamma} = \Omega R_1/(R_1 - R_2)$) in which Ω is the angular speed and R_1 and R_2 are the radii of the inner and out cylinders. This would be the standard results presented by the majority of the rheometers, but there are two main points that prevent us to use directly this approach. The first point is that the difference between the radii (the gap) is too large to use this approximation ($R_2/R_1 \approx 2.07$), which implies that we cannot treat the stress as uniform across the gap. The second point concerns the issue of shear banding briefly presented in the previous paper [19] in which it was shown that even after imposing high shear rates in the sample it is possible to observe an undeformed region in the gap. Based on these observations, and considering the strong stress variations in time of the material, we can conclude that it is important to have more information on the velocity distribution in the gap between the cylinders to be able to determine the rheological behavior of the material, as may be obtained by means of MRI.

3.2 Magnetic Resonance Velocimetry

The velocity profiles are measured during experiments following the same protocol as above (increasing then decreasing rotation velocity step range). The tangential velocity, *V*, is represented as a function of the distance. In order to observe the possible variations from one rotation velocity to another we rescaled the velocity by the maximum velocity, V_{max} (i.e. along the inner cylinder). The wall slip, an important concern in these system as reported by the Rheo-PIV measurements [17], was avoided by means of a rough surface in the cylinders. Comparing the velocity of the inner cylinder and the velocity of the fluid we can conclude that the wall slip was effectively negligible in our measurements. For the sake of clarity, in the different graphs, we present only the results associated with a few velocities during the increasing and decreasing phases. We carried out measurements during the first minute of flow and during the last minute of flow over five minutes. Each profile measurement lasts for 30 seconds. In some cases, there is a slight evolution of the velocity profile during the five minutes of shearing, which is illustrated in Figure 3 for one rotation velocity value. In the following we will leave apart this aspect and focus on the last velocity profile measured during the five minutes period at each rotation velocity.

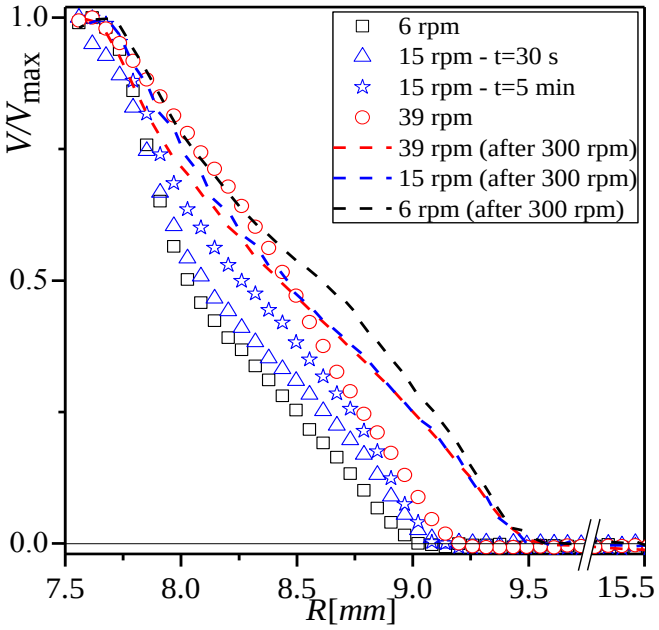

Figure 3. Dimensionless velocity (V/V_{max}) as a function of the radius for 7 wt.% of wax in oil. The symbols present the velocity profile during the increasing phase and the dashed lines present the velocity profile in the decreasing phase.

First, we focus on the data for the 7% concentration, which well illustrate different aspects. A first trend is that after flow start the material is sheared only in a band starting a fraction of millimeter from the inner cylinder and ending several millimeters from the outer cylinder (see Fig. 3). The existence of this unsheared region along the inner cylinder is surprising as the shear stress along the inner cylinder is the highest, which should induce flow preferentially to other regions. This suggests a thermal effect following the contact of the material with the cylinder, due to the heat conduction of the inner cylinder, which would induce a different solidification of the material close to it. However, the geometry is not metallic (Polypropylene) and we could check that the same result is obtained when all the system (geometry + sample) is heated in the oven before the test, which imposes a homogeneous cooling to the whole experiment. This suggests that this

unsheared region results from the conditions of breakage of the solid structure in the very first times, i.e. when the material is still in its solid (brittle) regime, a period during which the stress distribution does not necessarily follow the above simple relation (eq. 1) for the stress as a function of the torque and radius, as can be strictly derived only when the fluid flows symmetrically around the central axis. It is also possible that the thickness of this region slightly evolves during the increasing-decreasing rotation velocity sweep, but the resolution of our measurements does not allow to reach clear conclusions on this point. As a consequence, in the following, we will discuss essentially the evolution and shape of the velocity profile part beyond this unsheared region.

The existence of the outer unsheared region is expected for a simple yield stress fluid, as it can reflect the coexistence of sheared and unsheared regions, where the stress is respectively beyond and below the yield stress. However, two features show that this simple description is not sufficient here (see Fig. 3): (i) the sheared region thickness only increases marginally when the rotation velocity is significantly increased, and (ii) the shear rate in the liquid region along the liquid-solid interface strongly differs from zero. Moreover, the shear rate along this interface strongly increases with the rotation velocity, as may be concluded from the similar profile shape observed after rescaling (see Fig. 3). These different observations lead to conclude that the behavior of this material differs from that of a simple yield stress fluid [28] or a typical thixotropic fluid [23,29,30]. These aspects are in line with the knowledge that waxy oil suspensions are deformation-dependent "rheomalaxic" materials [31]. We will discuss these aspects in more details later on.

Let us look differently at these results: as a rough approximation we first consider the profiles as straight; under these conditions, we see that the material is sheared in a slightly growing region as the rotation velocity is increased up to 300 rpm; then the velocity profile is fixed when one decreases the rotation velocity. This means that, in conventional rheometry, the significant stress decrease observed during the increasing phase at each velocity level, does not correspond to a significant variation of the sheared thickness, but instead corresponds to a significant evolution of the structure of the flowing material, i.e, leading a decrease of the viscosity in the sheared layer. Then, after 300 rpm, the material structure has reached a state from which it does not evolve anymore during the decreasing phase, and finally we now get strictly the same (rescaled) profiles at different rotation velocities in that case. Actually, the superimposition of the rescaled velocity profiles in the decreasing phase tells us more on the rheological behavior of the fluid in this step. It may be demonstrated that in such a case the material composing the sheared region behaves as a power-law fluid (see [32]) as also noticed for crude oil and emulsions at different temperatures [33] . It is also worth emphasizing that this effect remains approximately true in time after a sudden change of velocity, which suggests that the material structure also keeps some similarity even during its transient evolution at a given rotation velocity level.

The exact shape of the velocity profiles, is in fact generally made of several parts of distinct slopes (see Fig. 5). This is likely the sign of some heterogeneity in the material, possibly due to some migration of the largest components towards the external part of the sheared region. As we do not have data about the density distribution we cannot elaborate further on this aspect. In the following we will neglect it and assume the material is homogeneous. This may induce some scattering on the data analysis, but does not affect the

general conclusions which rely on more important trends such as the constant thickness of the sheared layer and the similarity of the shape of the velocity profiles for different rotation velocities.

Let us now see how do the results vary with the concentrations. Similar results as those described above are obtained for a concentration of 8% (see Fig. 3b). For a lower concentration, 6%, close to the critical value for percolation (appearance of a solid structure, see [19]), we have similar trends but with a more significant evolution of the sheared thickness, especially during the step at 300 rpm (see Fig. 3a). Moreover, during the decreasing phase the velocity profiles are not perfectly similar after rescaling. Finally, for a concentration equal or larger than 10% the velocity varies rapidly over a very short distance (Fig. 3c and Appendix). For given boundary conditions we thus have a strong decrease of the sheared region thickness as the concentration increases from 6 to 15% (see Fig. 4). For the sake of quantitative comparison, the sheared region at the end of the first five minutes of shearing at 6 rpm is around 2.2, 1.9 and 0.5 mm for, respectively, 6, 8 and 12 wt% of wax content (see Fig. 4). Note that for a concentration larger than 10%, the thickness of the sheared layer is smaller than 1.0 mm which can be a concern regarding the continuum assumption. Indeed, in that case, the crystals present a needle-like structure with approximately a length of 100 μm for 10wt% and up to 400 μm for 12 and 15 wt.% of paraffin in oil (see Fig. A2 and ref. [19]) which gives a ratio of sheared thickness to particle size between 1 and 3, so of the order of particle size.

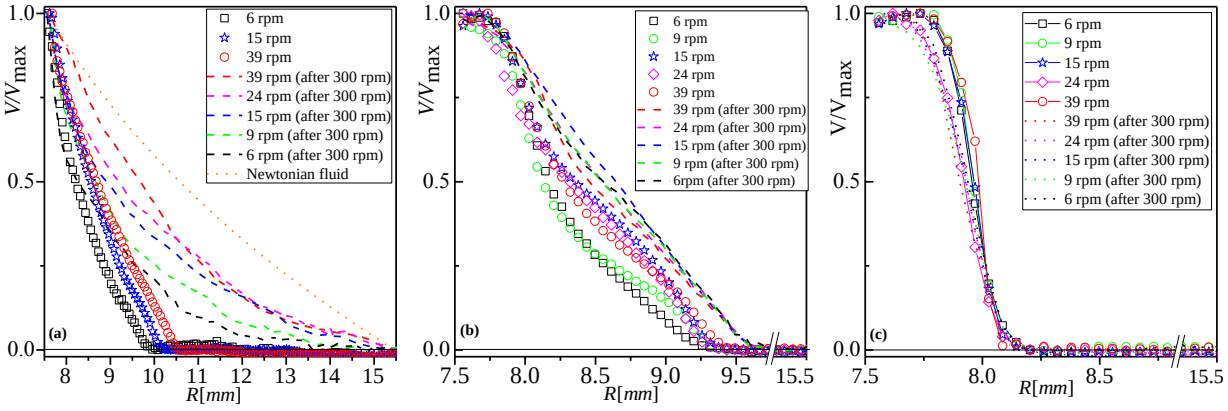

Figure 4. Dimensionless velocity (V/V_{max}) as a function of the radius for (a) 6wt%; (b) 8% and (c) 12%

Let us now discuss further the evolution of the sheared thickness. For a simple yield stress fluid, the thickness of the sheared region increases with the rotation velocity since the torque needed to induce flow is larger, so that according to the stress vs radius expression (eq. 1), the yield stress is reached at a larger distance (radius) from the inner cylinder. In addition, the shear rate in the liquid at the interface with the solid region tends to zero. The features of our fluids are thus strongly different from what is expected for a simple yield stress fluid. For a thixotropic yield stress fluid, we also expect a wider sheared region for an increasing rotation velocity if the material has been prepared in all cases by a preshear at a large velocity [23]. In that case the size of the sheared thickness corresponds to some balance between a restructuring process due to colloidal

interactions and a destructuring process imposed by shear, so that the critical shear rate along the interface is constant. These trends do not correspond to our observations here, as the sheared thickness does not significantly increase and the critical shear rate (along the interface) increases with the imposed rotation velocity. On the other side, if one imposes some rotation velocity (of the inner cylinder) to a material initially left at rest for a sufficient time, the result is more complex than above described, and a thinner shear layer may be obtained [23]. Indeed, in that case the material may have restructured and thus may exhibit a high yield stress, while after some flow leading to destructuring, the stress needed to impose a flow of the liquid layer may be still be significantly smaller than the yield stress of the material region still at rest. Under these conditions it is difficult to predict the size of the sheared layer, as it may depend on the start flow conditions; and if the yield stress of the unsheared region is sufficiently large its size will then not be much affected by some further increase of the rotation velocity of the inner cylinder. The effects observed here for the waxy suspensions seem to have some analogy with this (above) behavior. As soon as it has been formed during start flow at some given velocity, the sheared layer then marginally increases with the rotation velocity. This is consistent with the fact that the measured yield stress (from independent rheometrical tests) is much larger than the stress attained during our tests in most cases (except for 6%). Thus, as we increase the rotation velocity, we essentially further shear the currently liquefied layer (whose viscosity in general even further decrease) without affecting much the unsheared region. This implies that, during a protocol involving a progressive increase of the apparent shear rate followed by a decrease, the initially formed sheared layer, i.e. at the lowest imposed shear rate, governs the rest of the flow characteristics at different rotation velocities.

Note that for 7 and 8% we see some slight increase of the sheared thickness, despite the fact that the yield stress is still much larger than the stress even at 300 rpm. This might be due to some kind of progressive erosion of the solid region, a local effect which might require a smaller stress to play a significant role after a sufficient time of flow. For 6%, at the highest rotation velocity, the shear stress reaches values approximately in the same order of the material yields stress, then in this case it can be assumed that the stress induced by the flow is able to break-up the solid region and, consequently, increases the sheared region. In other words, here the shear banding widening effect (for this lowest concentration, 6%) can also be understood by a torque balance in which the effective shear stress overcomes the material yield stress and breaks the material in the unsheared region, widening the shear banding region.

We can analyze further these data by determining the apparent local behavior of the material. In that aim we can compute the local shear rate at each point of the velocity profiles. However, to limit the number of data points though still cover the full range of shear rates, for each profile we simply determine the shear rate in the middle of regions of approximately constant slope. Then we associate this shear rate to the shear stress in the middle of this slope (see example in Figure 5). In this figure, it is shown that we have three main regions/slopes (indicated by the lines in Figure 5) along the velocity profile. We then compute an effective shear stress ($\tau_{eff} = M/2\pi hR_m^2$) in each region, using the position in the middle of each slope, R_m. To compute the effective shear rate at the same point ($\dot{\gamma}_{eff} = -R_m\, d\omega/dr$) we use the development $\dot{\gamma}_{eff} = -dv_\theta/dr + v_{\theta,m}/R_m$, in which we introduce the slope dv_θ/dr of the profile in this region and the local tangential velocity, $v_{\theta,m}$.

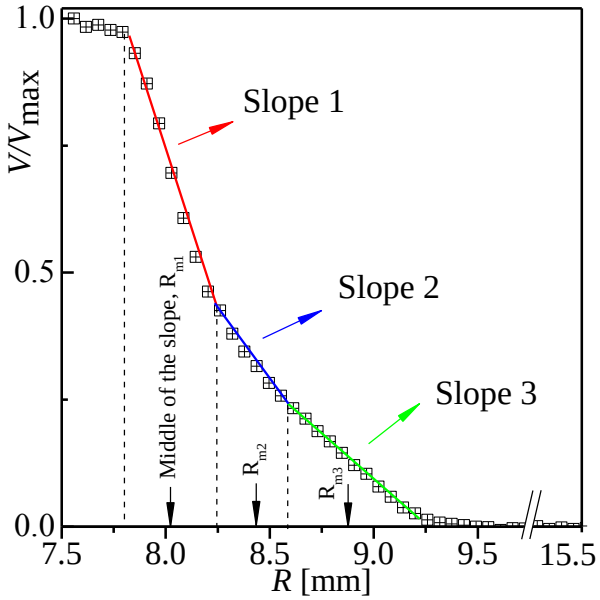

Figure 5. Dimensionless velocity (V/V_{max}) as a function of the radius (8 wt% and 6 RPM) and the slopes used to calculate the effective shear stress and the effective shear rate. The regions in the gap used to calculate the effective shear rate and the effective shear stress are defined as the sections in which there is a constant slope of the tangential velocity, v_θ, in the gap.

The results for the local stress vs shear rate data in the increasing phase show that, up to 10%, the material in the sheared region follows an apparent yield stress fluid behavior almost independent of the concentration (see Fig. 6a), except for 15% where the apparent behavior is qualitatively similar but situated at larger stress values (see Fig. 6a). This similarity of the constitutive equation means that, for such materials, under given boundary conditions, the major change in flow characteristics with the variation of the concentration is not the stress level to induce flow, but essentially the variation of the thickness of the sheared layer formed during the start flow (from rest) at a given velocity. It is nevertheless worth recalling that this behavior is the transient behavior of the material as the rotation velocity is progressively increased according to a fixed protocol for all concentrations, i.e. the data points at increasing shear rate correspond to the current behavior after five minutes of flow at the different, successive, rotation velocities.

A similar analysis was carried out for flow data obtained during the decreasing phase, which correspond to steady-state flows. Now all the data for the different concentrations in the range 6-15% fall along the same master curve, which exhibits a low apparent yield stress and tends to a power-law behavior at shear rates above 1 s^{-1} (see Fig. 6b). This confirms that the main change in flow characteristics with concentration is the size of the shear-band while the material behavior in this band is the same. Considering the large thickness variation, we can even say that, under steady-state flow conditions, the apparent rheological behavior of the material is governed by the size of the shear-band. Indeed, for example, for a given stress value, the ratio of shear rates observed for two different concentrations is approximately equal to the ratio of the sheared thicknesses, which can be up to 5 when the concentration is increased from 6 to 15%.

Actually, a simple liquid (Newtonian) behavior for these suspensions was suggested in [19] for some narrower range of concentrations, but here the analysis is done from direct measurements of the internal flow characteristics. A slightly larger viscosity is found here, by a factor about 1.5, which might be due to a difference between the maximum shear rate imposed in these two cases. The most important result here is that through this straightforward analysis of the flow characteristics we find a common rheological behavior of the liquid region at all concentrations in the range 6-15%. A Newtonian behavior is expected for suspensions in Newtonian fluid, but one also expects some variation with the concentration of suspended elements (see for example [34,35]), which does not appear here, possibly due the scattering on data. However, more striking is the fact that the same apparent viscosity is observed for the large concentrations (i.e. >10%) even when the sheared layer thickness is of the order of the size of the suspended elements. This implies that despite relatively complex properties leading in some cases to processes a priori not encompassed by the continuum assumption, the apparent behavior of the sheared regions remains rather simple.

The fact that, in the transient stages, the apparent viscosity is larger than the final one (steady state reached after high shear rate), can naturally result from the partial breakage of the structure. Indeed, if we simply assume that in these transient stages, aggregates of particles larger than the final ones exist in suspension, we deduce that due to the porosity of the aggregates a larger liquid volume fraction is embedded for larger aggregates, so that the concentration of solid elements (i.e. the aggregates) is larger (smaller liquid volume available for flow). Then any semi-empirical viscosity equations for suspensions as a function of the concentration and particle shape predict a higher viscosity in that case. Just after flow start, we likely have a suspension of large (porous) aggregates, which block a significant volume of liquid and give rise to a rather large apparent viscosity (since the apparent volume fraction of suspended elements is large). Then the size of these aggregates progressively decreases with shear intensity and/or time, which disperses more liquid and reduces the apparent solid concentration, which in turns decreases the apparent viscosity.

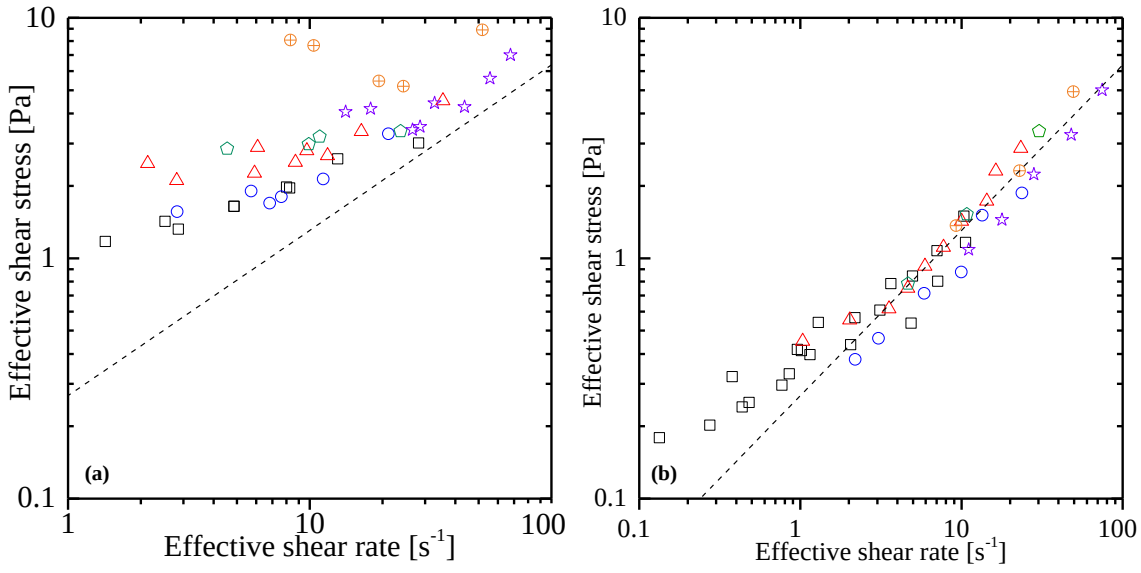

Figure 6. Effective shear stress as a function of the effective shear rate (a) increasing the rotation velocity and (b) decreasing the rotation velocity after imposing the maximum rotation of the equipment, for 6 %

(squares), 7% (circles), 8% (triangles), 10% (pentagons), 12% (stars) and 15% (cross-circles). The dashed line shows the behavior of a power-law fluid.

4. Summary of conclusions and consequences

Let us summarize our observations:

- Waxy oils can present an important shear banding effect, i.e. the coexistence of one region sheared at a finite shear rate and an unsheared region.
- In general, the size of this sheared region does not change much during an increasing ramp of velocity.
- Under given history of boundary conditions, the sheared region size increases when the concentration decreases, i.e. when the material yield stress decreases.
- As a consequence, this size depends on the initial flow conditions during start up flow and on the material yield stress.
- The behavior of the material in the sheared (liquid) region significantly varies in time; its apparent viscosity strongly decreases with time and/or imposed shear rate.
- This likely reflects the progressive breakage of the structure in smaller aggregates of particles, inducing a lower solid volume fraction of solid elements in suspension.
- The liquid region in steady state presents a power-law behavior, with a viscosity poorly dependent of the concentration.
- This result remains true even for large concentrations, when the thickness of the sheared region is of the order of the particle size.

Based on the results presented in this paper, mainly the point that the sheared thickness is a function of the strength of structured material at the end of the cooling, we can extrapolate the results to the pipeline restart flow. As we have shown for concentrations higher than the critical percolation concentration, the material breaks just in a small thickness of the gap. After the breakage, it seems that the material in the liquid regime is able to support the shear and, consequently, the unsheared region does not evolve or slightly evolves when higher shear rates are imposed in the sample. That implies that possibly in real pipelines conditions, at the moment of the start-up flow if the material presents a high yield stress (depending on the shear and thermal history) the breakage can happen just in a small region near to the walls of the pipe and after the breakage a plug-like flow can remain for a long time. It seems that even if a higher pump flow rate would be used to accelerate the flow, the plug-region should not reduce.

Some results presented in the literature can help us extrapolate this analysis. As discussed in the introduction, El-Gendy et al. [15] used a model waxy oil and by means of the PIV technique they presented the velocity profile of the material after the pipeline restart. In their case the inner diameter of the tube was around 13 mm and we can see that just a small portion of the material, with a thickness smaller than 0.5 mm, close to the walls was broken. A similar conclusion can be obtained for waxy crude oils analyzing results presented by Dalla et al. [36]. Looking at their results, first we can see that the abrupt flow after the breakage of the structure discussed for a model waxy oil in the previous paper [19] is also observed for the analyzed crude oil for

different thermal histories. Moreover, after the breakage the authors have taken pictures of the crude oil as a plug-like flowing out of the tube. By their figures, it seems that the higher the material yield stress the lower is the quantity of the crude oil that is in the liquid regime flowing out of the tube. It seems by these results that the findings of this paper can be extrapolated for pipeline conditions not only for model waxy oil but also in the crude oil scenarios.

Finally, these findings should have some impact of the analysis of the constitutive models proposed to simulate the rheological behavior of waxy oils, since we can conclude that in many cases the macroscopic results obtained by means of conventional rheometers are not representing the effective rheological behavior of the material because the unsheared region is not taken in consideration in these usual measurements. Although these models can get the main qualitative features of the transient behavior of waxy oils, further efforts have to be done to improve the experimental data available in the literature in order to validate the models in the liquid regime. On the other hand, determining the thickness of the unsheared region is still a tricking and open question. As a conclusion, it is important to emphasize the fact that we directly observe from these local measurements, the irreversible transition towards the liquid state, which precludes the use of standard thixoelastic models which fundamentally rely on the reversibility assumption. Then, our results finally suggest the need for developing specific models that would be able also to describe the shear-banding development in this irreversible context.

Acknowledgements

D.E.V.A acknowledges CAPES (Coordination for the Improvement of Higher Education Personnel - Brazil) (Process: 88881.170234/2018-01) for the Postdoctoral Fellowship.

Appendix

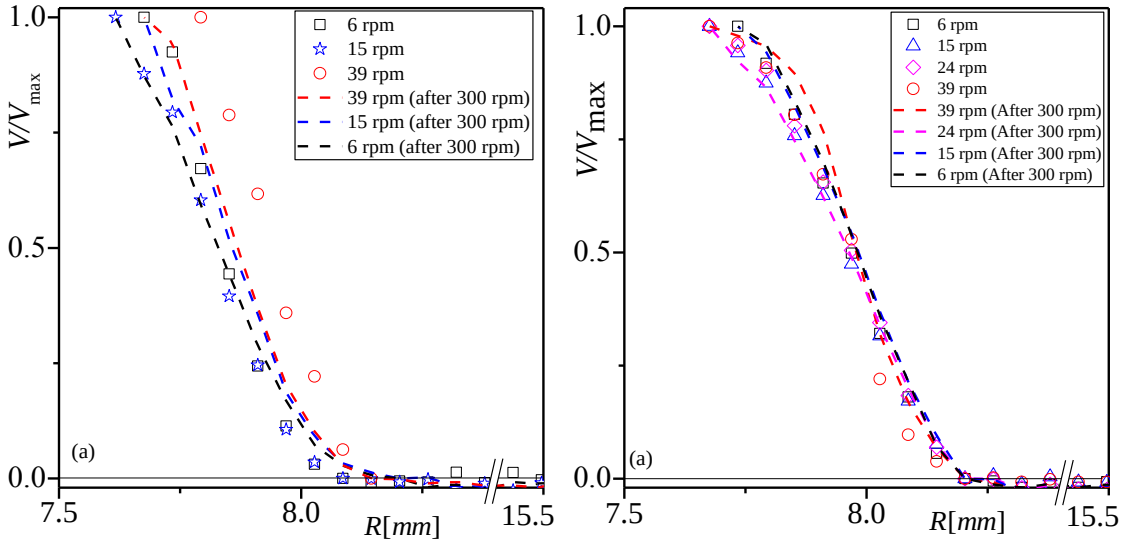

Figure A1. Dimensionless velocity (V/Vmax) as a function of the radius for (a) 10 wt.%; (b) 15 wt.%.

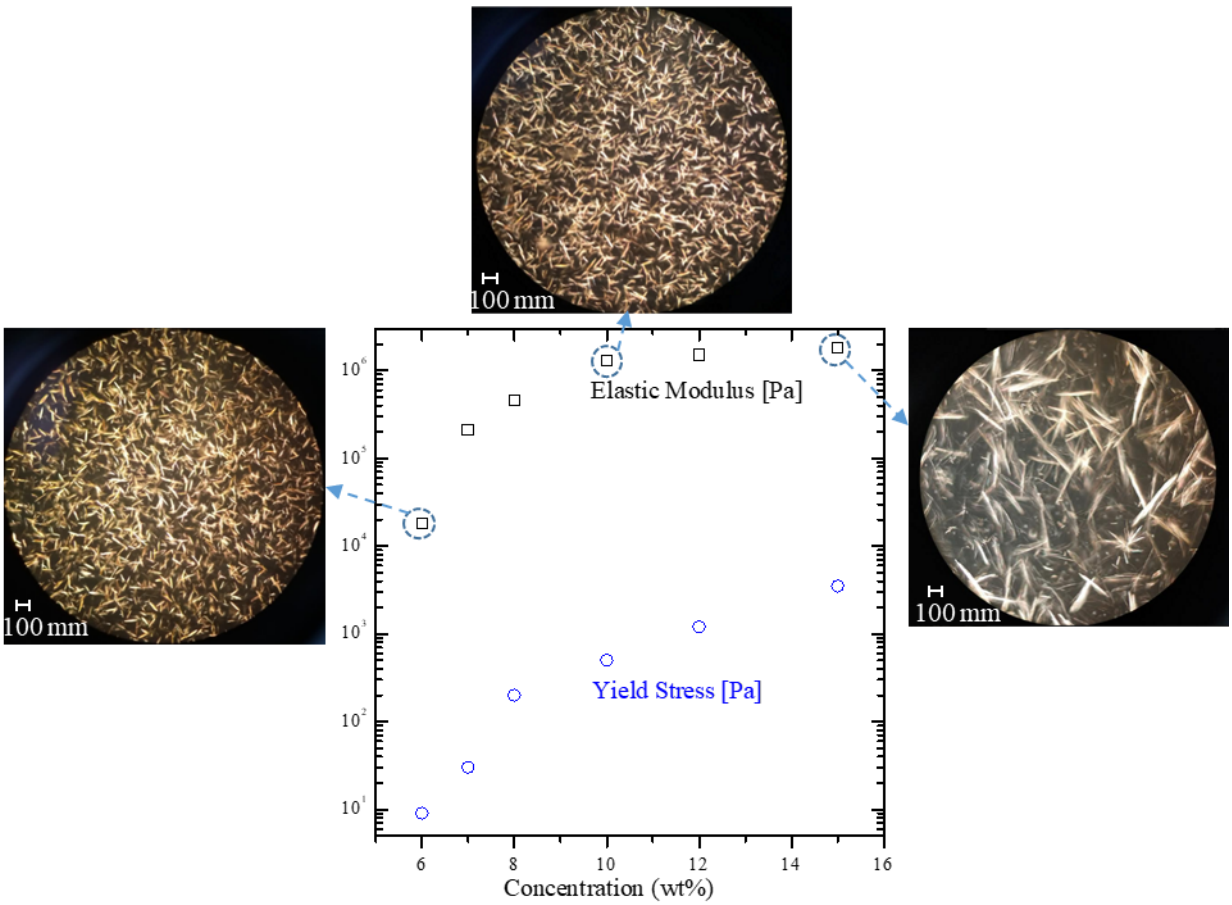

Figure A2 – Elastic modulus and yield stress as a function of the wax concentration. The Microscopic images show the crystals that form the structure in the solid regime. (Data from [19])

References

[1] R. Venkatesan, J.A. Östlund, H. Chawla, P. Wattana, M. Nydén, H.S. Fogler, The effect of Asphaltenes on the Gelation of Waxy Oils, Energy & Fuels. 17 (2003) 1630–1640. doi:10.1021/ef034013k.

[2] D.E.V. Andrade, A.C.B. da Cruz, A.T. Franco, C.O.R. Negrão, Influence of the initial cooling temperature on the gelation and yield stress of waxy crude oils, Rheol. Acta. 54 (2015) 149–157. doi:10.1007/s00397-014-0812-0.

[3] G.G. Vargas, E.J. Soares, R.L. Thompson, G.A.B. Sandoval, R.M. Andrade, F.B. Campos, A. Teixeira, Emulsion effects on the yield stress of gelled waxy crude oils, Fuel. 222 (2018) 444–456. doi:10.1016/j.fuel.2018.01.105.

[4] F.H. Marchesini, A.A. Alicke, P.R. de Souza Mendes, C.M. Ziglio, Rheological characterization of waxy crude oils: Sample preparation, Energy & Fuels. 26 (2012) 2566–2577.

[5] R.M. Webber, Low temperature rheology of lubricating mineral oils: Effects of cooling rate and wax crystallization on flow properties of base oils, J. Rheol. 43 (1999) 911–931. doi:10.1122/1.551045.

[6] D.E.V. Andrade, M.A. Marcelino Neto, C.O.R. Negrão, Non-monotonic response of waxy oil gel strength to cooling rate, Rheol. Acta. 57 (2018) 673–680. doi:10.1007/s00397-018-1108-6.

[7] R. Venkatesan, N.R. Nagarajan, K. Paso, Y.B. Yi, A.M. Sastry, H.S. Fogler, The strength of paraffin gels formed under static and flow conditions, Chem. Eng. Sci. 60 (2005) 3587–3598. doi:10.1016/j.ces.2005.02.045.

[8] I.M. El-Gamal, Combined effects of shear and flow improvers: The optimum solution for handling waxy crudes below pour point, Colloids Surfaces A Physicochem. Eng. Asp. 135 (1998) 283–291. doi:10.1016/S0927-7757(97)00261-6.

[9] D.E.V. Andrade, M.A. Marcelino Neto, C.O.R. Negrão, The importance of supersaturation on determining the solid-liquid equilibrium temperature of waxy oils, Fuel. 206 (2017) 516–523. doi:10.1016/j.fuel.2017.06.042.

[10] R.F.G. Visintin, R. Lapasin, E. Vignati, P. D'Antona, T.P. Lockhart, Rheological behavior and structural interpretation of waxy crude oil gels, Langmuir. 21 (2005) 6240–6249. doi:10.1021/la050705k.

[11] J.A. Lopes-da-Silva, J.A.P. Coutinho, Analysis of the isothermal structure development in waxy crude oils under quiescent conditions, Energy & Fuels. 21 (2007) 3612–3617. doi:10.1021/ef700357v.

[12] H.S. Lee, P. Singh, W.H. Thomason, H.S. Fogler, Waxy oil gel breaking mechanisms: Adhesive versus cohesive failure, Energy & Fuels. 22 (2008) 480–487. doi:10.1021/ef700212v.

[13] H.P. Rønningsen, B. Bjorndal, A.B. Hansen, W.B. Pedersen, Wax precipitation from North Sea crude oils. 1. Crystallization and dissolution temperatures, and Newtonian and non-Newtonian flow properties, Energy & Fuels. 5 (1991) 895–908. doi:10.1021/ef00030a019.

[14] F. Yang, B. Yao, C. Li, G. Sun, X. Ma, Oil dispersible polymethylsilsesquioxane (PMSQ) microspheres improve the flow behavior of waxy crude oil through spacial hindrance effect, Fuel. 199 (2017) 4–13. doi:10.1016/j.fuel.2017.02.062.

[15] H. El-Gendy, M. Alcoutlabi, M. Jemmett, M. Deo, J. Magda, R. Venkatesan, A. Montesi, The propagation of pressure in a gelled waxy oil pipeline as studied by particle imaging velocimetry, AIChE J. 58 (2012) 302–311. doi:10.1002/aic.12560.

[16] C.J. Dimitriou, G.H. McKinley, A comprehensive constitutive law for waxy crude oil: a thixotropic yield stress fluid., Soft Matter. 10 (2014) 6619–44. doi:10.1039/c4sm00578c.

[17] C.J. Dimitriou, G.H. McKinley, R. Venkatesan, Rheo-PIV analysis of the yielding and flow of model waxy crude oils, Energy & Fuels. 25 (2011) 3040–3052. doi:10.1021/ef2002348.

[18] R. Mendes, G. Vinay, G. Ovarlez, P. Coussot, Reversible and irreversible destructuring flow in waxy oils: An MRI study, J. Non - Newton. Fluid Mech. 220 (2015) 77–86. doi:10.1016/j.jnnfm.2014.09.011.

[19] D.E.V. Andrade, P. Coussot, Brittle solid collapse to simple liquid for a waxy suspension, Soft Matter. 15 (2019) 8766–8777. doi:10.1039/c9sm01517e.

[20] G. Ovarlez, S. Cohen-Addad, K. Krishan, J. Goyon, P. Coussot, On the existence of a simple yield stress fluid behavior, J. Nonnewton. Fluid Mech. 193 (2013) 68–79. doi:10.1016/j.jnnfm.2012.06.009.

[21] S. Rodts, J. Boujlel, B. Rabideau, G. Ovarlez, N. Roussel, P. Moucheront, C. Lanos, F. Bertrand, P. Coussot, Solid-liquid transition and rejuvenation similarities in complex flows of thixotropic materials studied by NMR and MRI, (2010) 1–15. doi:10.1103/PhysRevE.81.021402.

[22] A. Ragouilliaux, B. Herzhaft, F. Bertrand, P. Coussot, Flow instability and shear localization in a drilling mud, Rheol. Acta. 46 (2006) 261–271. doi:10.1007/s00397-006-0114-2.

[23] J.S. Raynaud, P. Moucheront, J.C. Baudez, F. Bertrand, J.P. Guilbaud, P. Coussot, Direct determination by nuclear magnetic resonance of the thixotropic and yielding behavior of suspensions, J. Rheol. (N. Y. N. Y). 46 (2002) 709–732. doi:10.1122/1.1463420.

[24] M.C. Khalil De Oliveira, M.A. Gonçalves, An effort to establish correlations between brazilian crude oils properties and flow assurance related issues, Energy & Fuels. 26 (2012) 5689–5701. doi:10.1021/ef300650k.

[25] I.A. Frigaard, K.G. Paso, P.R. de Souza Mendes, Bingham's model in the oil and gas industry, Rheol. Acta. (2017) 259–282. doi:10.1007/s00397-017-0999-y.

[26] A.D. Hanlon, S.J. Gibbs, L.D. Hall, D.E. Haycock, W.J. Frith, S. Ablett, Rapid MRI and Velocimetry of Cylindrical Couette Flow, Magn. Reson. Imaging. 16 (1998) 953–961. doi:https://doi.org/10.1016/S0730-725X(98)00089-7.

[27] X. Zhang, T. Oerther, M. Ferrari, P. Basset, F. Rouyer, J. Goyon, E. Lorenceau, T. Bourouina, P. Coussot, Wall slip mechanisms in direct and inverse emulsions, J. Rheol. (N. Y. N. Y). 62 (2018) 1495–1513. doi:10.1122/1.5046893.

[28] P. Coussot, L. Tocquer, C. Lanos, G. Ovarlez, Macroscopic vs. local rheology of yield stress fluids, J. Nonnewton. Fluid Mech. 158 (2009) 85–90. doi:10.1016/j.jnnfm.2008.08.003.

[29] P. Coussot, J.S. Raynaud, F. Bertrand, P. Moucheront, J.P. Guilbaud, H.T. Huynh, S. Jarny, D. Lesueur, Coexistence of liquid and solid phases in flowing soft-glassy materials, Phys. Rev. Lett. 88 (2002) 2183011–2183014. doi:10.1103/PhysRevLett.88.218301.

[30] G. Ovarlez, S. Rodts, X. Chateau, P. Coussot, Phenomenology and physical origin of shear localization and shear banding in complex fluids, Rheol. Acta. 48 (2009) 831–844. doi:10.1007/s00397-008-0344-6.

[31] S. Rodriguez-Fabia, R. Lopez Fyllingsnes, N. Winter-Hjelm, J. Norrman, K.G. Paso, Influence of Measuring Geometry on Rheomalaxis of Macrocrystalline Wax-Oil Gels: Alteration of Breakage Mechanism from Adhesive to Cohesive, Energy and Fuels. 33 (2019) 654–664. doi:10.1021/acs.energyfuels.8b02725.

[32] P. Coussot, Rheometry of pastes, suspensions and granular materials: Applications in industry and environment, John Wiley & Sons, Inc., Hoboken, NJ, USA, 2005.

[33] K. Paso, A. Silset, G. Soørland, M.D. a L. Gonçalves, J. Sjöblom, Characterization of the formation, flowability, and resolution of brazilian crude oil emulsions, Energy & Fuels. 23 (2009) 471–480. doi:10.1021/ef800585s.

[34] I.M. Krieger, T.J. Dougherty, A Mechanism for Non- Newtonian Flow in Suspensions of Rigid Spheres, Trans. Soc. Rheol. 3 (1959) 137–152. doi:10.1122/1.548848.

[35] T. Kitano, T. Kataoka, T. Shirota, An empirical equation of the relative viscosity of polymer melts filled with various inorganic fillers, Rheol. Acta. 20 (1981) 207–209. doi:10.1007/BF01513064.

[36] L.F.R. Dalla, E.J. Soares, R.N. Siqueira, Start-up of waxy crude oils in pipelines, J. Nonnewton. Fluid Mech. 263 (2019) 61–68. doi:10.1016/j.jnnfm.2018.11.008.